Crossover from Localized to Cascade Relaxations in Metallic Glasses

Yue Fan, Takuya Iwashita, and Takeshi Egami

Crossover from localized to cascade relaxations in metallic glasses

Yue Fan[1,*], Takuya Iwashita[2], and Takeshi Egami[1,2,3]

[1]Materials Science and Technology Division, Oak Ridge National Laboratory, Oak Ridge, Tennessee 37831, USA

[2]Department of Physics and Astronomy, Joint Institute for Neutron Sciences, and [3]Department of Materials Science and Engineering, University of Tennessee, Knoxville, Tennessee 37996, USA

Corresponding author email:fany@ornl.gov

Abstract

Thermally activated deformation is investigated in two metallic glass systems with different cooling histories. By probing the atomic displacements and stresses changes on the potential energy landscape (PEL), two deformation modes—localized process and cascade process—have been observed. The localized deformation involves less than 30 atoms, appears in both systems, and its size is invariant of cooling history. However, the cascade deformation is more frequently observed in the fast quenched system than in the slowly quenched system. The origin of the cascade process in the fast quenched system is attributed to the higher density of local minima on the underlying PEL.

Deformation in amorphous system is believed to occur through local rearrangement of a group of atoms, known as the shear transformation zones (STZs) [1-5]. While the behaviors of STZs under external strain-driven condition (*e.g.* athermal quasistatic (AQS) limit) have been extensively investigated[6-9], the atomistic mechanisms of STZs' nucleation and relaxation under thermal excitation, as well as the interplays between thermal activation and external shear still remain as open challenges[10]. Recently Rodney *et al*[10, 11] and Derlet *et al*[12, 13] have made significant progress in understanding thermally activated plasticity in glasses based on the concept of potential energy landscape (PEL). In the present study, we focus our scope on the structures of underlying PEL in metallic glasses, particularly on how the PEL is affected by thermal processing history (*i.e.* cooling rates during glass formation), and how the mechanisms of thermally activated deformation is influenced by it.
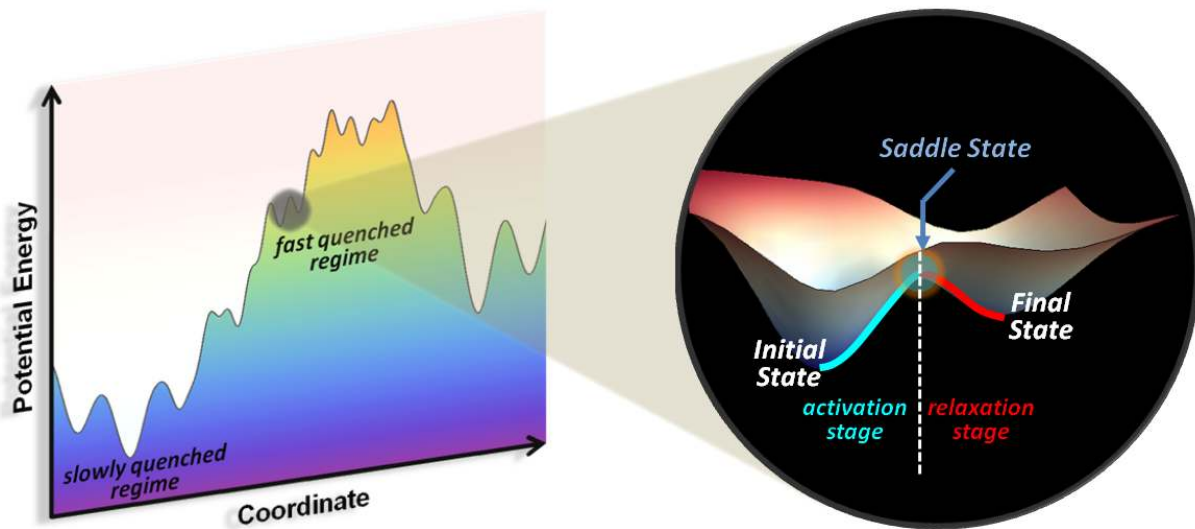

Figure 1: A schematic illustration on potential energy landscape (PEL) and an elementary deformation process from the perspective of PEL.

In the perspective of PEL[14, 15], elementary deformation units are identified as the hopping between the neighboring "sub-basins" confined within a "meta-basin"[16-18], termed

β relaxations, whereas the transitions between "meta-basins", also known as α relaxations, correspond to percolation of β relaxations[19] and lead to macroscopic plastic flow in glasses. As illustrated in Fig.1, the elementary deformation process consists of two key stages: namely the activation stage (from the initial states to the nearby saddle states), and the relaxation stage (from the saddle states to the final states). The former stage constitutes the trigger mechanism of STZs[20], while the latter stage determines the response of the system to accommodate the relaxation of STZs. To identify the saddle states and the final states, we employ the activation-relaxation technique (ART)[21, 22]—known to be capable of providing representative PEL samplings in amorphous systems[11, 23]—to a well-known metallic glass model system $Cu_{56}Zr_{44}$[24]. To study thermally activated deformation, initial perturbations are introduced to a small group of atoms with local connectivity[25], which are then followed by the searching algorithm in ART[22] to identify the deformation pathways, including both the saddles states and the final states. In order to directly compare the similarities and differences between the activation stages and relaxation stages, we use the same model employed in our previous study[20]. The size of the simulation box is 32.43Å $\times$ 32.43Å $\times$ 32.43Å, containing 2000 atoms. We employ an embedded-atom method (EAM) potential[24], with periodic boundary conditions applied to all directions (more details in [26]). To probe the aging history effects on the thermally activated deformation, we prepared two starting models with different cooling rates. System I is produced by making an instant quench to 0K from the high temperature liquid at 2000K ($\sim 3T_g$, where T_g is the glass transition temperature), and therefore represents an unstable system. System II is prepared at finite cooling rate (1K/ps) from an equilibrated low temperature liquid at 1000K ($\sim 1.5T_g$) to a glass, and thus represents a relatively more stable system. In total around 4,500 distinct deformation pathways have been identified by ART method. No external

loads have been applied in the simulation, because the present study concerns thermally activated deformation.

The relations between atomic stress changes and atomic displacements have been demonstrated effective in identifying the important atoms during deformation[20, 31]. In this study the atomic level stress tensor[32-34] for each atom was calculated at the initial state ($\sigma_{i,ini}^{\alpha\beta}$), the saddle state ($\sigma_{i,sad}^{\alpha\beta}$), and the final state ($\sigma_{i,fin}^{\alpha\beta}$), respectively. The stress change for each atom at the saddle state and the final state are thus given by $\Delta\sigma_i^{\alpha\beta}(sad) = \sigma_{i,sad}^{\alpha\beta} - \sigma_{i,ini}^{\alpha\beta}$, and $\Delta\sigma_i^{\alpha\beta}(fin) = \sigma_{i,fin}^{\alpha\beta} - \sigma_{i,ini}^{\alpha\beta}$, respectively. The von Mises stress change for each atom can be calculated as,

$$\Delta\sigma_{VM}^i = \sqrt{\frac{1}{2}\left[\left(\Delta\sigma_i^{11} - \Delta\sigma_i^{22}\right)^2 + \left(\Delta\sigma_i^{22} - \Delta\sigma_i^{33}\right)^2 + \left(\Delta\sigma_i^{33} - \Delta\sigma_i^{11}\right)^2 + 6\left(\Delta^2\sigma_i^{12} + \Delta^2\sigma_i^{23} + \Delta^2\sigma_i^{31}\right)\right]}$$

Fig.2.a shows the atomic stress changes and displacements of each atom at the saddle state and the final state, for one typical elementary deformation identified by ART. It is observed that the vast majority of atoms have only small displacements and stress changes, with a linear correlation (solid blue line in Fig.2.a). However, a small number of atoms (outside the shadow region in Fig.2.a) exhibit significant deviations, and are the important particles involved in the deformation[20, 35]. It can be seen that during deformation, more atoms are involved in the final state than in the saddle state. Apparently, in reaching the final state, rearrangements of more atoms are necessary to accommodate the relaxation[20, 31].
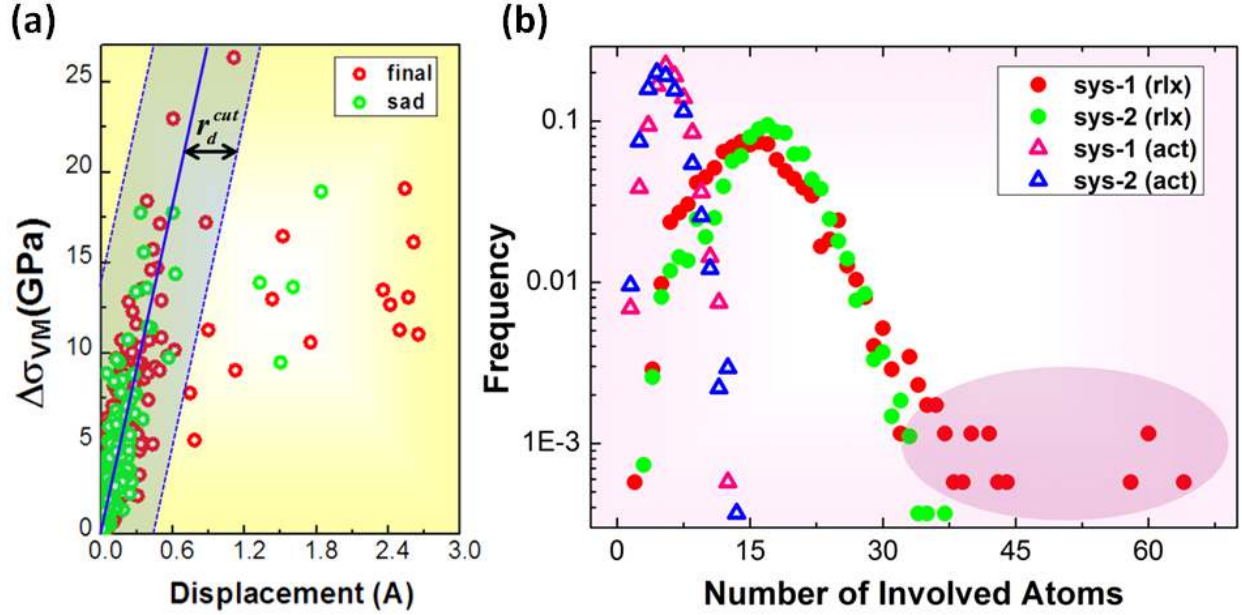
Figure 2: (a) The relation between the atomic displacements and the stress changes at saddle (green open circle) and final (red open circle) states, for a typical deformation process. (b) The distributions of the number of involved atoms during activation stage (denoted as "*act*") at saddle states, and after relaxation stage at (denoted as "*rlx*") at final states, respectively. The distributions of two systems are the same at saddle states, while at final states SYS-I exhibits a long tail, related with cascades. A typical visualization of cascade in SYS-I is shown in [26].

The number of important atoms can be measured by removing background fluctuations with an appropriate cut-off distance r_d^{cut} shown in Fig.2.a (details in [26]). Fig.2.b shows the size distributions of the involved atoms, for all 4,500 saddle states and final states in the two systems. During the activation stage (i.e. at the saddle states, denoted as "*act*" in the legend of Fig.2.b), there are only about 5 atoms participated in the STZ triggers (triangles in Fig.2.b), which are consistent with the studies by Demkowicz and Argon[31, 36]. More importantly, the size distributions in SYS-I and SYS-II are almost identical to each other at the saddle states, indicating the deformation triggers are independent of the systems' cooling histories[20].

After the relaxation stage (i.e. at the final states, denoted as "*rlx*" in the legend of Fig.2.b), the average size increases to around 17, which is consistent with reported STZs sizes (from 10 to

30 atoms) measured in a number of experiments[37-41] and simulations[4, 8, 35, 42, 43]. It is worth noting that, the size distributions of SYS-I and SYS-II overlap well at relatively small sizes (less than 30 atoms), suggesting a system-independent deformation mechanism in this regime.

On the other hand, very importantly, the size distributions of SYS-I and SYS-II show considerable differences at large sizes (greater than 30 atoms). The fast quenched SYS-I displays a long-tail distribution (shadowed region in Fig.2.b) up to around 65 atoms, which seems to suggest SYS-I is more susceptible to cascades than SYS-II during the relaxation stage. We further checked the effects of boundary conditions on the results, and found that constant-pressure simulations also led to the same behavior (seen in [26]).

The scaling relations between the barrier heights and the path lengths on PEL can help reveal the underlying nature of deformation[44, 45]. It has been demonstrated according to a catastrophe theory that, in many-body interacting systems, there exists a universal scaling relation, $E \sim d^2$, between the local PEL minima and the neighboring saddle states, where E represents the barrier height and d is the path length[36, 37]. Note that *for local transitions between neighboring sub-basins*, according to the symmetry, both the forward barriers (i.e. energy differences between the initial and saddle states) and the reverse barriers (i.e. energy differences between the final and saddle states) yield the same scaling relation with path lengths. The relations between forward barriers and path lengths have been demonstrated to follow the same scaling in both SYS-I and SYS-II, indicating the deformation trigger mechanisms (i.e. the activation stage) are localized and independent of the system's thermal history. On the other hand, however, the behaviors of the two systems during relaxation stage are significantly different.
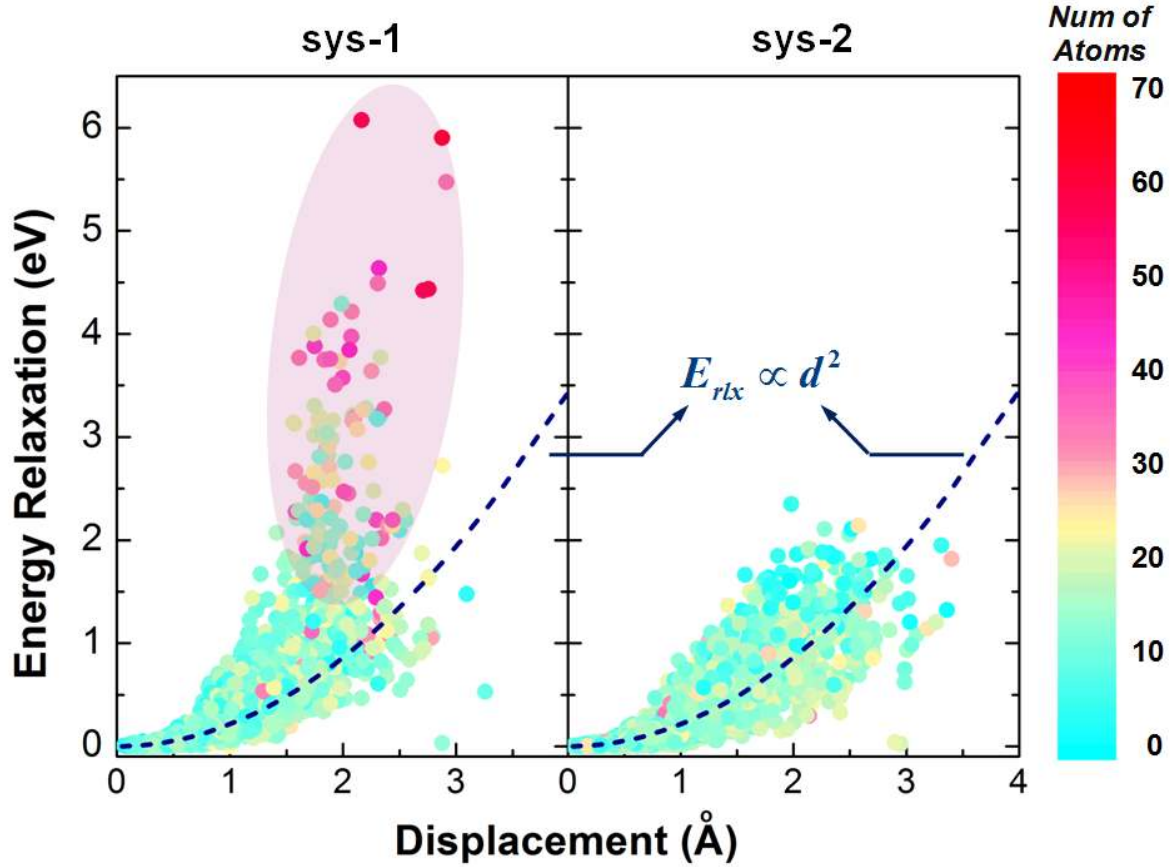
Figure 3: The relations between energy relaxations and maximum atomic displacements (from saddle to final states), in SYS-I and SYS-II. The dashed curves represent the scaling relation for localized transition predicted by catastrophe theory[36, 37], where E_{rlx} refers to the energy relaxation and d refers to the displacement. The color of each point is associated with the number of involved atoms, which can be read from the color bar on the right side. It can be seen that SYS-II contains only the localized relaxation with small size. However, SYS-I includes an extra non-local relaxation mode associated with larger size.

Fig.3 shows the relations between the energy of relaxation (i.e. energy differences between the final and saddle states) and the maximum atomic displacements which represents effective path length during the relaxation. Each data point is colored according to the number of involved atoms after the relaxation shown in Fig.2.b. It can be seen that most data points in SYS-I and almost all data points in SYS-II follow the same scaling, $E \sim d^2$ (E_{rlx} in Fig.3 refers to the energy relaxation), indicating a system-independent localized relaxation mode, for the deformation associated with sizes smaller than 30 atoms.

8

However in the fast quenched SYS-I, in addition to the localized mode, there exists another branch of relaxation (shadowed region in Fig.3). The extra branch significantly deviates from the scaling, $E \sim d^2$, and therefore represents a non-local relaxation pattern. Such non-local mode in SYS-I leads to larger magnitude of energy relaxation (up to 6 eV) than the localized relaxation in SYS-II (less than 2 eV). In addition, the non-local branch in SYS-I is associated with larger number of atoms, and exactly corresponds to the long-tail in Fig.2.b. In other words, the thermally activated deformation with the sizes larger than 30 atoms is non-localized, and seems to include cascade behaviors (note that here the size of 30 atoms is based on metallic glass systems, and some quantitative differences might occur for other amorphous materials such as oxide glasses, a-silicon, etc). While we believe the non-local events may also exist in SYS-II, they are apparently much rarer than in SYS-I so that we did not observe them given the present system size.
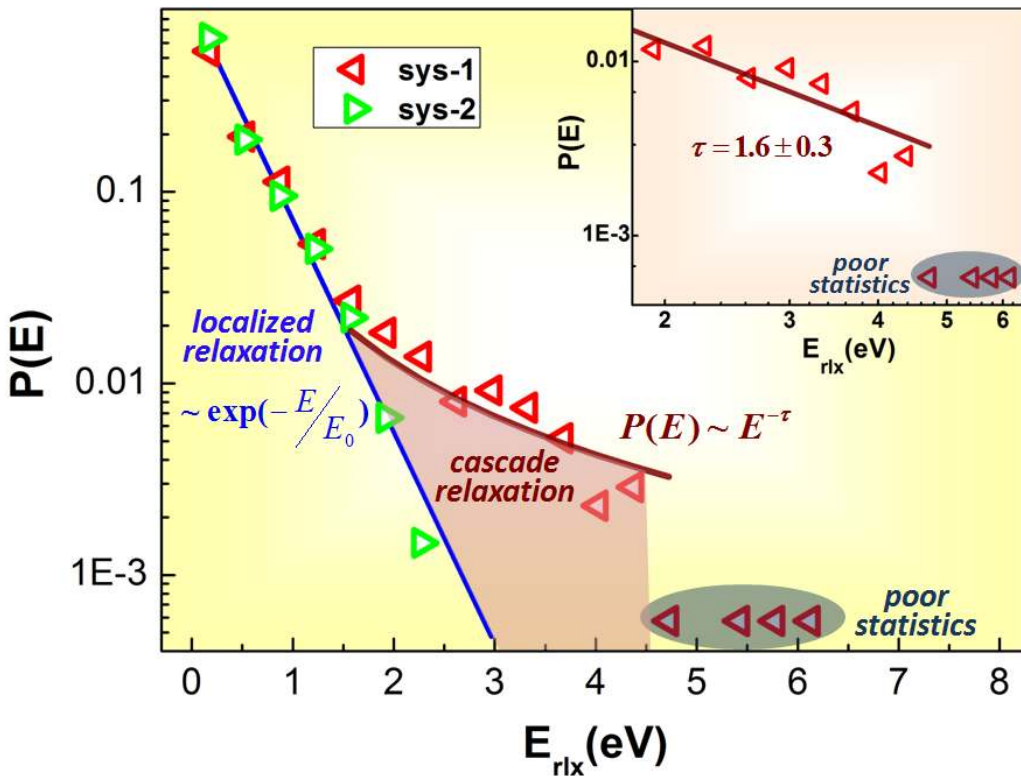

9

Figure 4: The distributions of energy relaxations (denoted as E_{rlx} in x-axis) in SYS-I (red triangles) and SYS-II (green triangles). SYS-II shows an exponential decay over the entire regime, indicating a localized relaxation mode. SYS-I shows a mixture of exponential decay (at small energy regime) and power law decay (at large energy regime), suggesting a combination of localized and cascade relaxations. Inset: The log-log plot for the power law decay in SYS-I. The critical exponent is calculated as 1.6, which represents a typical cascade behavior.

We further calculated the distributions of the energy of relaxation (i.e. energy differences between the final and saddle states) in both systems, as seen in Fig.4. In SYS-II, the probability shows an exponential decay behavior (blue line), with a characteristic energy relaxation of E_0 : 0.32 eV. As has been noted by Demkowicz, Argon[24, 29], and Bailey et al[46], the fast exponential decay indicates a localized process, which is well consistent with the analysis above. In SYS-I, the distribution at small energy regime shows the similar exponential decay. This is because below 2 eV, as seen in Fig.3, the non-local branch does not appear in SYS-I yet. However at larger magnitude of energy relaxation, SYS-I shows much slower power-law decay. Note that there are only few stochastic data points at very large energy relaxation, which yield very small probability in the order of 10^{-4}. These few data points have poor statistics, and thus were not used in the power-law fitting, following previous convention[47, 48]. Further analysis (inset of Fig.4) provides an exponent of 1.6 for the power-law decay. Such fractal dimension suggests a typical self-organized criticality (i.e. cascade behavior), which has been universally observed in many different systems[36, 47, 49, 50]. However it is worth noting that, the range of log-log plot in the inset of Fig.4 is quite small, and the deduced exponent should be subject to further examination for larger systems.

In glassy materials, when the systems are mechanically driven to the steady state of flow, the power-law cascades have been observed from both experiments[51] and simulations[48]. However thermally induced cascades seen in SYS-I without external shear, to the best of our

knowledge, have not been reported before. We believe the crossover from localized relaxations to cascades seen in SYS-I stems from the structure of underlying PEL of the system. In particular, the path lengths between neighboring minima on PEL are much shorter in a less stable system (SYS-I) than in a more stable system (SYS-II)[20], which consequently yields a much higher density of local PEL minima in SYS-I than in SYS-II[14, 20]. This is consistent with recent experiments[52], which demonstrated that the density of regions more prone to shear deformation is significantly higher in a less relaxed system when comparing with a better annealed system. As a result, the higher density of local PEL minima states makes SYS-I more susceptible to cascades. Therefore in addition to the localized relaxations with small energy drops, sometimes the relaxations can go wild[53] and induce cascades because the neighboring PEL minima are too close to each other in SYS-I. This explains the non-local branch in Fig.3 and the power-law decay in Fig.4.

To summarize, the present study investigated the relaxation stages during thermally activated deformation in metallic glasses. We observed a localized relaxation mode involving around 17 atoms, which is independent of the system's thermal history. On the other hand the fast quenched SYS-I contains an extra relaxation process, which has much larger sizes, involving up to 65 atoms. Further analyses demonstrate that the energy relaxation of the extra mode in SYS-I exhibits a power-law decay with the exponent of 1.6, close to the value of *D/2*, where *D* denotes dimension, universally observed in many different avalanche systems[47, 49, 50]. Such a power-law suggests a typical self-organized criticality, demonstrating the extra mode in SYS-I is essentially a *cascade behavior*.

The crossover from localized relaxations to cascades seen in SYS-I originates from the underlying PEL structures. SYS-I is more susceptible to cascades because the fast quenched

SYS-I has a much higher density of local minima on PEL than the more slowly quenched SYS-II[20]. Therefore sometimes local deformation in SYS-I can initiate avalanches, involving more atoms and yielding a typical cascade behavior. Admittedly, there are new questions remains to be answered. For example, when glassy materials are driven under external shear at low temperatures[48, 51], only the power-law cascades appear, while the localized relaxations have not been observed. Such discrepancy suggests that there are noticeable differences between the thermally activated deformation and external shear induced deformation[10, 11, 54], which would warrant further studies.

References:

[1]   A. S. Argon, *"Plastic deformation in metallic glasses"*, *Acta Metallurgica* **27** (1979) 47.

[2]   A. S. Argon, and H. Y. Kuo, *"Plastic flow in a disordered bubble raft (an analog of a metallic glass)"*, *Materials Science and Engineering* **39** (1979) 101.

[3]   H.-B. Yu, W.-H. Wang, and K. Samwer, *"The β relaxation in metallic glasses: an overview"*, *Materials Today* **16** (2013) 183.

[4]   M. L. Falk, and J. S. Langer, *"Dynamics of viscoplastic deformation in amorphous solids"*, *Physical Review E* **57** (1998) 7192.

[5]   C. A. Schuh, T. C. Hufnagel, and U. Ramamurty, *"Mechanical behavior of amorphous alloys"*, *Acta Materialia* **55** (2007) 4067.

[6]   M. Tsamados, A. Tanguy, C. Goldenberg, and J.-L. Barrat, *"Local elasticity map and plasticity in a model Lennard-Jones glass"*, *Physical Review E* **80** (2009) 026112.

[7]   C. E. Maloney, and A. Lemaître, *"Amorphous systems in athermal, quasistatic shear"*, *Physical Review E* **74** (2006) 016118.

[8]   C. A. Schuh, and A. C. Lund, *"Atomistic basis for the plastic yield criterion of metallic glass"*, *Nature Materials* **2** (2003) 449.

[9]   M. L. Manning, and A. J. Liu, *"Vibrational Modes Identify Soft Spots in a Sheared Disordered Packing"*, *Physical Review Letters* **107** (2011) 108302.

[10]   D. Rodney, A. Tanguy, and D. Vandembroucq, *"Modeling the mechanics of amorphous solids at different length scale and time scale"*, *Modelling and Simulation in Materials Science and Engineering* **19** (2011) 083001.

[11]   D. Rodney, and C. Schuh, *"Distribution of Thermally Activated Plastic Events in a Flowing Glass"*, *Physical Review Letters* **102** (2009) 235503.

[12]   P. M. Derlet, and R. Maaß, *"Thermal-activation model for freezing and the elastic robustness of bulk metallic glasses"*, *Physical Review B* **84** (2011) 220201.

[13]   P. M. Derlet, and R. Maaß, *"Linking high- and low-temperature plasticity in bulk metallic glasses: thermal activation, extreme value statistics and kinetic freezing"*, *Philosophical Magazine* **93** (2013) 4232.

[14]   F. H. Stillinger, *"A Topographic View of Supercooled Liquids and Glass Formation"*, *Science* **267** (1995) 1935.

[15]   P. G. Debenedetti, and F. H. Stillinger, *"Supercooled liquids and the glass transition"*, *Nature* **410** (2001) 259.

[16]   G. P. Johari, and M. Goldstein, *"Viscous Liquids and the Glass Transition. II. Secondary Relaxations in Glasses of Rigid Molecules"*, *The Journal of Chemical Physics* **53** (1970) 2372.

[17]   W. L. Johnson, and K. Samwer, *"A Universal Criterion for Plastic Yielding of Metallic Glasses with a (T/T_{g})^{2/3} Temperature Dependence"*, *Physical Review Letters* **95** (2005) 195501.

[18]   S. G. Mayr, *"Activation Energy of Shear Transformation Zones: A Key for Understanding Rheology of Glasses and Liquids"*, *Physical Review Letters* **97** (2006) 195501.

[19]   J. S. Harmon, M. D. Demetriou, W. L. Johnson, and K. Samwer, *"Anelastic to Plastic Transition in Metallic Glass-Forming Liquids"*, *Physical Review Letters* **99** (2007) 135502.

[20]   Y. Fan, T. Iwashita, and T. Egami, *"How thermally activated deformation starts in metallic glass"*, *Nature Communications* **5** (2014) 5083.

[21]   G. T. Barkema, and N. Mousseau, *"Event-based relaxation of continuous disordered systems"*, *Physical Review Letters* **77** (1996) 4358.

[22]   E. Cances *et al.*, *"Some improvements of the activation-relaxation technique method for finding transition pathways on potential energy surfaces"*, *Journal of Chemical Physics* **130** (2009) 114711.

[23]   H. Kallel, N. Mousseau, and F. Schiettekatte, *"Evolution of the Potential-Energy Surface of Amorphous Silicon"*, *Physical Review Letters* **105** (2010) 045503.

[24]   Y. Q. Cheng, E. Ma, and H. W. Sheng, *"Atomic Level Structure in Multicomponent Bulk Metallic Glass"*, *Physical Review Letters* **102** (2009) 245501.

[25]   T. Iwashita, D. M. Nicholson, and T. Egami, *"Elementary Excitations and Crossover Phenomenon in Liquids"*, *Physical Review Letters* **110** (2013) 205504.

[26]   See Supplementary Material, which includes Refs.[27-30]

[27]   J. Caris, and J. J. Lewandowski, *"Pressure effects on metallic glasses"*, *Acta Materialia* **58** (2010) 1026.

[28]   P. Lowhaphandu, S. L. Montgomery, and J. J. Lewandowski, *"Effects of superimposed hydrostatic pressure on flow and fracture of a Zr-Ti-Ni-Cu-Be bulk amorphous alloy"*, *Scripta Materialia* **41** (1999) 19.

[29]   W. Dmowski *et al.*, *"Universal mechanism of thermomechanical deformation in metallic glasses"*, *Physical Review B* **91** (2015) 060101.

[30]   Y. Q. Cheng, and E. Ma, *"Atomic-level structure and structure–property relationship in metallic glasses"*, *Progress in Materials Science* **56** (2011) 379.

[31]   M. J. Demkowicz, and A. S. Argon, *"Autocatalytic avalanches of unit inelastic shearing events are the mechanism of plastic deformation in amorphous silicon"*, *Physical Review B* **72** (2005) 245206.

[32]   T. Egami, K. Maeda, and V. Vitek, *"Structural defects in amorphous solids A computer simulation study"*, *Philosophical Magazine A* **41** (1980) 883.

[33]   T. Egami, and D. Srolovitz, *"Local structural fluctuations in amorphous and liquid metals: a simple theory of the glass transition"*, *Journal of Physics F: Metal Physics* **12** (1982) 2141.

[34]   Y. Fan, T. Iwashita, and T. Egami, *"Evolution of elastic heterogeneity during aging in metallic glasses"*, *Physical Review E* **89** (2014) 062313.

[35]   F. Delogu, *"Identification and Characterization of Potential Shear Transformation Zones in Metallic Glasses"*, *Physical Review Letters* **100** (2008) 255901.

[36]   A. S. Argon, *"Strain avalanches in plasticity"*, *Philosophical Magazine* (2013) 1.

[37]   C. A. Schuh, A. C. Lund, and T. G. Nieh, *"New regime of homogeneous flow in the deformation map of metallic glasses: elevated temperature nanoindentation experiments and mechanistic modeling"*, *Acta Materialia* **52** (2004) 5879.

[38]   J. D. Ju, D. Jang, A. Nwankpa, and M. Atzmon, *"An atomically quantized hierarchy of shear transformation zones in a metallic glass"*, *Journal of Applied Physics* **109** (2011) 053522.

[39]   I.-C. Choi *et al.*, *"Estimation of the shear transformation zone size in a bulk metallic glass through statistical analysis of the first pop-in stresses during spherical nanoindentation"*, *Scripta Materialia* **66** (2012) 923.

[40]   J. D. Ju, and M. Atzmon, *"A comprehensive atomistic analysis of the experimental dynamic-mechanical response of a metallic glass"*, *Acta Materialia* **74** (2014) 183.

[41]   M. Atzmon, and J. D. Ju, *"Microscopic description of flow defects and relaxation in metallic glasses"*, *Physical Review E* **90** (2014) 042313.

[42]   M. L. Falk, *"Molecular-dynamics study of ductile and brittle fracture in model noncrystalline solids"*, *Physical Review B* **60** (1999) 7062.

[43]   A. C. Lund, and C. A. Schuh, *"Yield surface of a simulated metallic glass"*, *Acta Materialia* **51** (2003) 5399.

[44]   D. J. Wales, *"A Microscopic Basis for the Global Appearance of Energy Landscapes"*, *Science* **293** (2001) 2067.

[45]   D. J. Wales, *"Decoding the energy landscape: extracting structure, dynamics and thermodynamics"*, *Philosophical Transactions of the Royal Society A: Mathematical, Physical and Engineering Sciences* **370** (2012) 2877.

[46]   N. P. Bailey, T. B. Schrøder, and J. C. Dyre, *"Exponential Distributions of Collective Flow-Event Properties in Viscous Liquid Dynamics"*, *Physical Review Letters* **102** (2009) 055701.

[47]   M. C. Miguel *et al.*, *"Intermittent dislocation flow in viscoplastic deformation"*, *Nature* **410** (2001) 667.

[48]   K. M. Salerno, C. E. Maloney, and M. O. Robbins, *"Avalanches in Strained Amorphous Solids: Does Inertia Destroy Critical Behavior?"*, *Physical Review Letters* **109** (2012) 105703.

[49]   J. P. Sethna, K. A. Dahmen, and C. R. Myers, *"Crackling noise"*, *Nature* **410** (2001) 242.

[50]   G. Durin, and S. Zapperi, *"Scaling Exponents for Barkhausen Avalanches in Polycrystalline and Amorphous Ferromagnets"*, *Physical Review Letters* **84** (2000) 4705.

[51]   J.-O. Krisponeit *et al.*, *"Crossover from random three-dimensional avalanches to correlated nano shear bands in metallic glasses"*, *Nat Commun* **5** (2014).

[52]   W. Li *et al.*, *"Structural heterogeneity induced plasticity in bulk metallic glasses: From well-relaxed fragile glass to metal-like behavior"*, *Applied Physics Letters* **103** (2013).

[53]   L. Liu *et al.*, *"Direct observation of hierarchical nucleation of martensite and size-dependent superelasticity in shape memory alloys"*, *Nanoscale* **6** (2014) 2067.

[54]   P. Cao, H. S. Park, and X. Lin, *"Strain-rate and temperature-driven transition in the shear transformation zone for two-dimensional amorphous solids"*, *Physical Review E* **88** (2013) 042404.